ОБЪЕДИНЕННЫЙ
ИНСТИТУТ
ЯДЕРНЫХ
ИССЛЕДОВАНИЙ
ДУБНА

E1 - 11653

E.Balea, S.Berceanu, C.Coca,
V.M.Karnaukhov, G.Kellner, A.Mihul,
V.I.Moroz, A.Sararu, V.K.Volchkov

Ξ^- AND $\bar{\Xi}^+$ PRODUCTION IN π^-p INTERACTIONS AT 16 GEV/C

1978

E1 - 11653

E.Balea,[1] S.Berceanu,[1] C.Coca,[1]
V.M.Karnaukhov, G.Kellner,[3] A.Mihul,[2]
V.I.Moroz, A.Sararu,[1] V.K.Volchkov

Ξ^- AND $\bar{\Xi}^+$ PRODUCTION IN π^-p INTERACTIONS AT 16 GEV/C

Submitted to "Nuclear Physics"

1 *Institute of Nuclear Physics and Engineering, Bucharest.*
2 *University of Bucharest.*
3 *CERN, Geneva.*

Баля Е. и др. **E1 - 11653**

Ξ^- и $\bar{\Xi}^+$-гипероны в π^-p-взаимодействиях при 16 ГэВ/с

Ξ^- и $\bar{\Xi}^+$-гипероны изучались в π^-p-взаимодействиях при 16 ГэВ/с. Даны сечения для Ξ^- и $\bar{\Xi}^+$-частиц. Представлены распределения и средние величины углов, поперечных и продольных импульсов в с.ц.м. Представлены также характеристики некоторых идентифицированных финальных состояний с Ξ-частицами.

Работа выполнена в Лаборатории вычислительной техники и автоматизации ОИЯИ.

Препринт Объединенного института ядерных исследований. Дубна 1978

Balea E. et al. **E1 - 11653**

Ξ^- and $\bar{\Xi}^+$ Production in π^-p Interactions at 16 GeV/c

Production of Ξ^- and $\bar{\Xi}^+$ hyperons has been studied in 16 GeV/c π^-p interactions. The cross sections are given for Ξ^- and $\bar{\Xi}^+$ production. Distributions and average values of c.m. production angle, transverse and longitudinal variables are presented. The characteristics of some Ξ final states identified are also presented.

The investigation has been performed at the Laborytory of Computing Techniques,and Automation, JINR.

Preprint of the Joint Institute for Nuclear Research. Dubna 1978

1. INTRODUCTION

The data for this experiment come from about 120.000 pictures obtained from three exposures of the 2m CERN hydrogen bubble chamber to a separated π^- beam having momenta of 15.850, 16.275 amd 16.295 GeV/c,respectively, at the chamber center.

We reported here only on the production of Ξ^- and $\bar{\Xi}^+$ particles. The procedure for identifying and analysing the V° type events, as well as some results concerning the cross sections for production of neutral strange particles in these interactions are given in ref.[1] and some references therein.

In section 2 we discuss the procedures for analysing the data. Results on the cross section determination are given in section 3. General characteristics of Ξ's in c.m. system and some average values for different parameters are presented in section 4.Characteristics of the Ξ production channels are separately treated in the last section.

2. SAMPLE SELECTION AND WEIGHTING

The film was scanned twice for all primary interactions, within a central fiducial volume with at least an associated V°- or

$V^{\pm}$-decay indicating strange particles in the final states. In the regular scan of the film, events that indicated a possible cascade decay (e.g., topology with a V°-decay pointing to a kink in a secondary track and which lay on the opposite side of the secondary track from the deflected track) were compiled into a list of cascade decay participants. All the events collected were measured on the digitized microscopes and geometrically reconstructed [2]. The identification of V°'s was performed on the basis of a kinematical fitting [3]. The events having a Λ° or $\bar{\Lambda}^{\circ}$ associated with a kink were then processed through all the selection criteria of a cascade decay $\Xi^- \to \Lambda^{\circ}\pi^-$ and $\bar{\Xi}^+ \to \Lambda^{\circ}\pi^+$. A check for consistency with track ionization has been also done.

Finally 46 events which had a Λ° associated with a negative kink and 3 events, having a $\bar{\Lambda}^{\circ}$ associated with a positive kink, were identified as charged Ξ decays.

We have estimated the mass and lifetime of Ξ^-'s, in order to test the quality of our sample of events. The average value of the mass is found to be $M_{\Xi^-} = 1320.60 \pm 0.63$ MeV. The lifetime for Ξ^-'s determined from our data is $c\tau = 4.11 \pm 0.56$ cm.

Both these values are consistent with world averages.

The observed number of Ξ events was weighted by a total weight, representing the product of different weights obtained as follows:

1. In order to allow for loss of events due to (a) imposing the minimum length cut-off of decaying particles and (b) their escape from the finite fiducial volume, each

observed decaying particle (Ξ and Λ° from Ξ decay) was given a weight

$$W = [\exp(-\frac{L_{min}}{L_0 \cos\lambda}) - \exp(-\frac{L_{pot}}{L_0})]^{-1},$$

where L_{pot} is the distance from the production vertex to the edge of the decay fiducial volume along the particle direction, L_{min} is the minimum projected cut-off length appropriate to the type of particle (in this experiment the limits were fixed at: $L_{min} = 0.2$ cm for Ξ's and $L_{min} = 0.3$ cm for Λ's, in the observation plane), L_0 is the mean decay length ($L_0 = \frac{P}{m} c\tau$, where m and τ are respectively the mass and lifetime of particle, and p is the measured momentum) and λ is the Ξ dip angle.

The average values obtained for all Ξ's and Λ°'s are $\bar{W}_{\Xi} = 1.060 \pm 0.022$ and $\bar{W}_{\Lambda^{\circ}} = 1.184 \pm 0.036$, respectively.

2. A weight, W_{θ} is associated with discarding all $\Xi^-(\bar{\Xi}^+)$ events, having a projected decay angle θ_p less than 3°, where a cut was made. This weight has been determined from the analytical form of the weight function of the observed Ξ decay which is a function depending only on the projection of the Ξ's momentum, for a given θ_p (see ref. [4]). In order to obtain the θ_p value proper to our experiment, we calculated the number of Ξ's weighted by W_{θ} for different θ_p between 1.0 and 10.0°, cutting events for which the projection angle was smaller than the assumed θ_p. The calculated numbers are given as a function of θ_p in fig. 1. The θ_p cut-off chosen, 3°, is such that from there the number of weighted Ξ becomes almost constant.

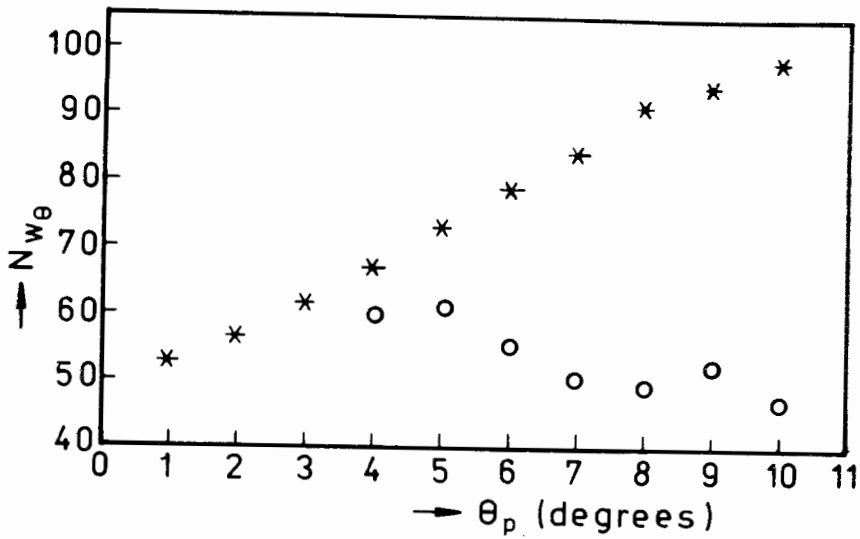

Fig. 1. Weighted number of Ξ events as a function of the cut in projected angle.

The average value obtained for W_θ is

$\bar{W}_\theta = 1.273 \pm 0.034$

3. Number of weighted events has still been scaled by the branching fractions for $\Lambda^\circ(\bar{\Lambda}^\circ)$.

4. A correction is made, too, for the scanning losses (1.04 for 2-prong events and 1.01 for events of higher multiplicity).

Table 1 lists the observed number of Ξ events as well as the corrected one, as a function of topology.

As it can be seen from table 1 the average multiplicity of charged particles in events with visible Ξ hyperons is

$\langle n \rangle = 3.82 \pm 0.22$.

Table 1

Cross sections for Ξ^- and $\bar{\Xi}^+$ production in π^-p interactions at 16 GeV/c

n_{ch}	number of observed Ξ^-	Corrected number	σ^{ch}_n (μb)	$\langle n_{\Xi^-} \rangle$ per inelastic interaction	Number of observed $\bar{\Xi}^+$	Corrected number	σ^{ch}_n (μb)
2	I6	34.8	5.I±I.3	0.00094±0.00024	2	5.9±4.2	0.87±0.68
4	I9	54.6	8.I±I.9	0.00080±0.00027	I	$2.0^{+4.6}_{-I.6}$	$0.29^{+0.67}_{-0.24}$
6	I0	25.3	3.7±I.2	0.00077±0.00025	0	0	-
8	I	3.9	$0.6^{+I.3}_{-0.5}$	$0.00042^{+0.00096}_{-0.00033}$	0	0	-
Total	46	II8.6	I7.5±2.7	0.00082±0.00013	3	7.9±4.6	I.2±0.7

3. CROSS SECTION RESULTS

The cross sections have been calculated by normalization on the total $\pi^- p$ cross section at 16 GeV/c interpolated from measurements obtained in counter experiments [5]. The sample of events used here corresponds to a "cross section per event" of 0.1477 ± ±0.0058 μb/event.

The total cross sections for Ξ^- and $\bar{\Xi}^+$ produced by π^- at 16 GeV/c have been found to be: $\sigma_{\Xi^-} = 17.51 \pm 2.72 \mu b$ and $\sigma_{\bar{\Xi}^+} = 1.16 \pm 0.67 \mu b$, respectively.

Table 1 lists the values for Ξ^- and $\bar{\Xi}^+$ production cross sections for different multiplicities of charged prongs.

Figure 2 displays the Ξ^- topological cross sections as function of charged topology, togerher with the average numbers of Ξ^-'s per inelastic $\pi^- p$ interactions. $\langle n_{\Xi^-} \rangle$ seems to decrease slowly with increasing n_{ch}.

The average number obtained for $\bar{\Xi}^+$'s per inelastic $\pi^- p$ collisions is very small ($\langle n_{\bar{\Xi}^+} \rangle = 0.000054 \pm 0.000031$).

The data available for the variation of Ξ^- production cross section in $\pi^- p$ interactions with the value of the incoming momentum in the lab. system are summarized in fig. 3. The line drown through the experimental points is only to guide the eye.

4. MOMENTUM AND ANGULAR DEPENDENCES. AVERAGE VALUES

The dependence of the Ξ^- production cross section on the X and p_T^2 variables is shown in figs. 4 and 5. Figure 4 plots $F_1(x)$ as

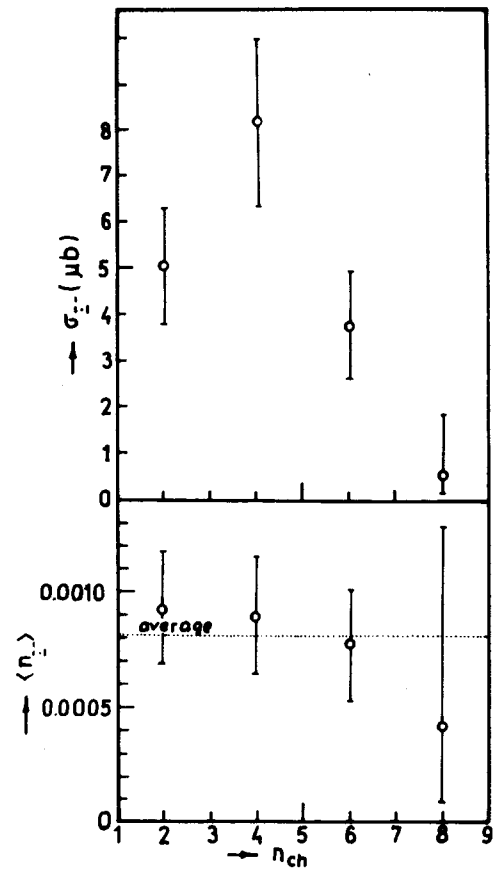

Fig. 2. Cross section for Ξ^- production and average number of Ξ^-'s, ($\langle n_{\Xi^-} \rangle$), produced per inelastic $\pi^- p$ collisions as functions of charge multiplicity.

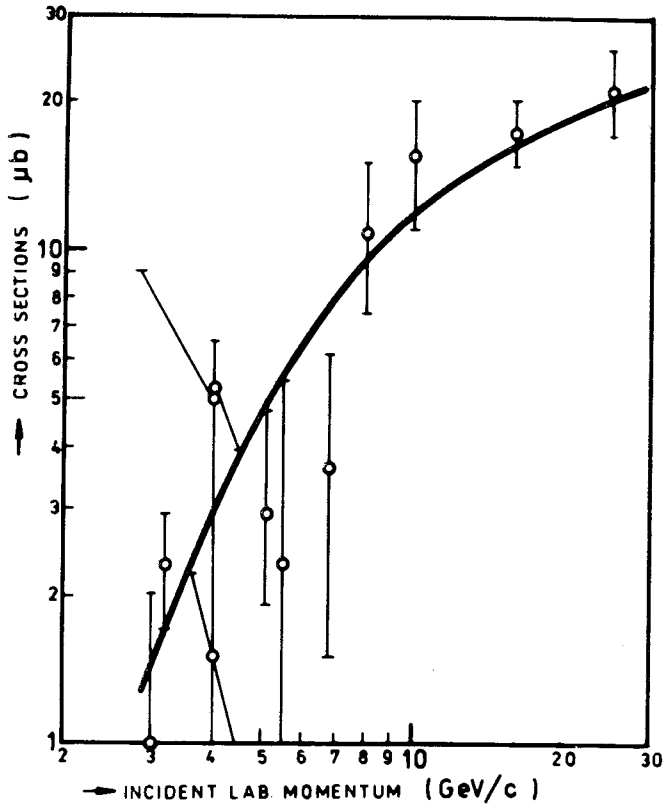

Fig. 3. Cross section for Ξ^- production in π^-p reactions as function of incident momentum.

a function of the Feynman variable

$$F_1(x) = \frac{2}{\pi\sqrt{s}} \int \frac{E^* d^2\sigma}{dx\, dp_T^2} dp_T^2,$$

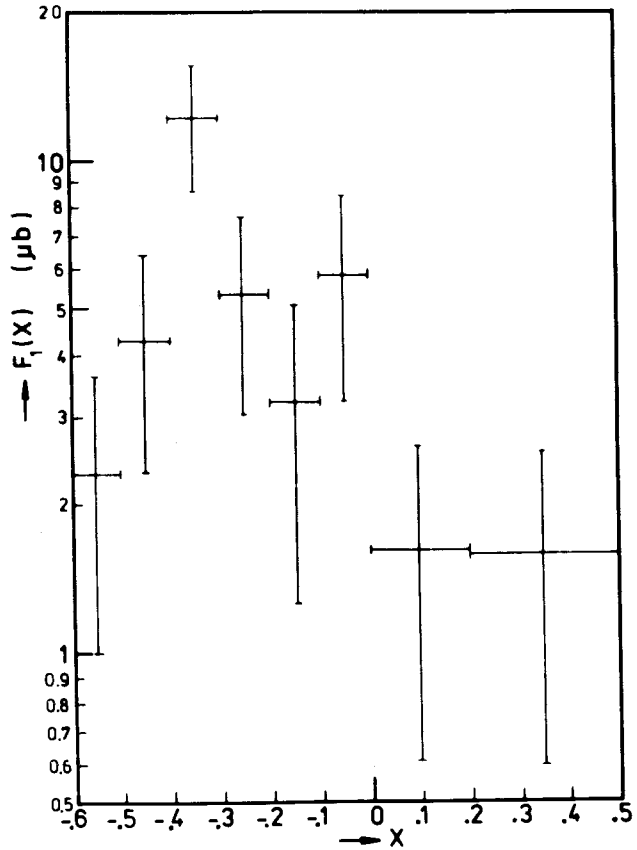

Fig. 4. $F_1(x)$ as a function of x for Ξ^- production.

where

$$x = \frac{2P_L^*}{\sqrt{s}}$$

(all quantities are calculated in the center of mass).

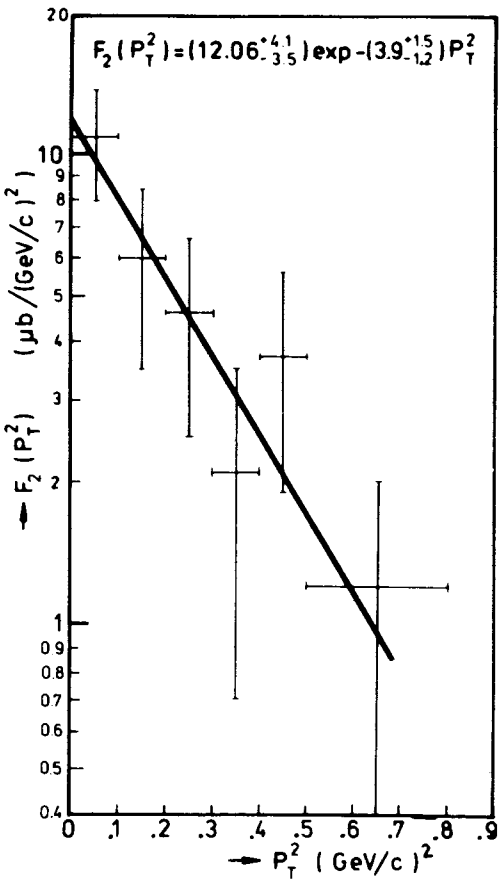

Fig. 5. $F_2(p_T^2)$ as a function of p_T^2 for Ξ^- production.

Note that Ξ^- production is peaked preferentially in the backward direction.

Figure 5 shows $F_2(p_T^2)$ as a function of p_T^2 for Ξ^-'s

$$F_2(p_T^2) = \frac{2}{\pi\sqrt{s}} \int \frac{E^* d^2\sigma}{dx\, dp_T^2} dx.$$

F_2 - distribution shows the usual exponential behaviour at small p_T^2. The solid line represents a single exponential fit to the data of the form $A \exp(-BP_T^2)$ for $0 < P_T^2 < 0.65$ (GeV/c)^2. The parameters of the fit are $A = 12.06^{+4.16}_{-3.52}$ (μb/(GeV/c)^2) and $B = 3.89^{+1.50}_{-1.20}$ (GeV/c)$^{-2}$ with a χ^2 of 1.49 for three degrees of freedom.

Figure 6 gives the plot $P_T - P_L^*$ with its different projections for all Ξ^-'s produced. The $3\bar{\Xi}^+$ produced are also indicated in this figure (cross hatched). As is seen in fig. 6 the transverse momenta of the Ξ's are limited, almost all Ξ's falling in the region below 1 GeV/c. P_L^* distribution, like the invariant x-distribution, shows that Ξ^-'s are mostly grouped backwards with negative value of P_L^*. This effect is very pronounced for Ξ^-'s produced in 2-prong events. However, there is an excess of Ξ^-'s in the forward hemisphere produced mostly in 4-prong events. From the angular distribution we find a large accumulation of events in the very backward direction for the Ξ^-'s ($\cos\theta^* < -0.8$). The total forward-backward asymmetry parameter $A(A = B-F/B+F)$ is found to be $A = 0.56 \pm 0.12$.

Table 2 summarizes some average values obtained for different variables for Ξ^-'s as functions of the multiplicity of charged particles.

In table 3 the forward-backward asymmetry, A, is given for Ξ^-'s produced by π^- of different incident momenta. As is seen in table 3, A decreases with increasing incident momentum.

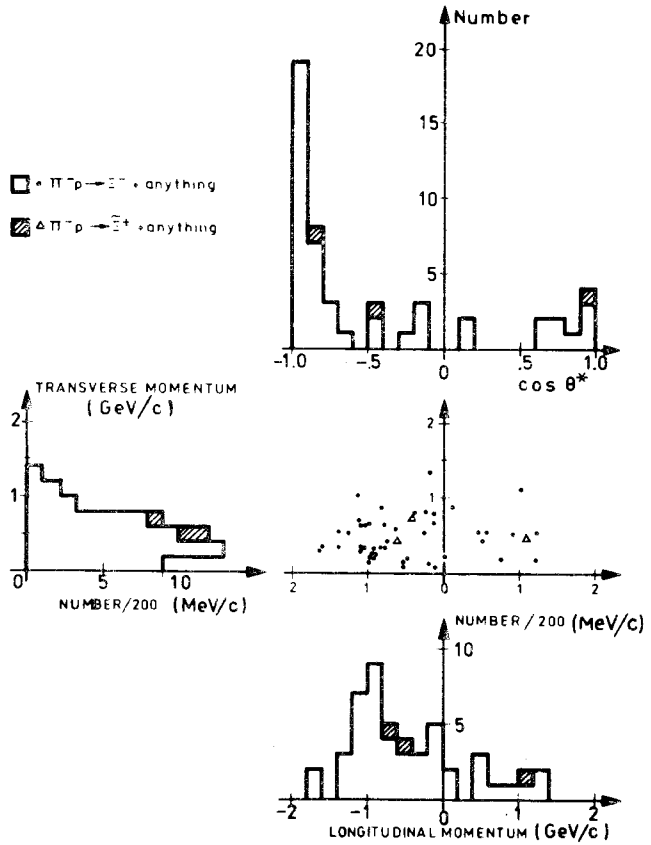

Fig. 6. Plot of P_T versus P_L^* for all Ξ's produced and projections of their $\cos\theta^*, P_L^*$ and P_T distributions.

As poor as statistics are for $\bar{\Xi}^+$'s, no clear difference in their behaviour compared with that of the Ξ^-'s could be seen in fig. 6.

Table 2

C.m. average values for Ξ^-'s produced in π^-p interactions, as functions of charge multiplicity

n_{ch} / average values	2	4	6	Total
$\langle \cos\theta^* \rangle$	−0.847 ± 0.057	−0.169 ± 0.177	−0.588 ± 0.181	−0.473 ± 0.099
$\langle P_L^* \rangle$	−0.895 ± 0.108	−0.099 ± 0.178	−0.696 ± 0.206	−0.483 ± 0.111
$\langle x \rangle$	−0.322 ± 0.039	−0.036 ± 0.064	−0.250 ± 0.074	−0.174 ± 0.040
$\langle P_T \rangle$	0.400 ± 0.050	0.510 ± 0.072	0.514 ± 0.114	0.473 ± 0.042
$\langle P_T^2 \rangle$	0.198 ± 0.042	0.355 ± 0.083	0.381 ± 0.170	0.304 ± 0.052
$\langle x \rangle_E$	−0.339 ± 0.042	−0.033 ± 0.075	−0.265 ± 0.081	−0.185 ± 0.052
$\langle P_T^2 \rangle_E$	0.203 ± 0.045	0.386 ± 0.097	0.386 ± 0.192	0.319 ± 0.061

Table 3

Forward-backward asymmetry parameter

Incident momentum (GeV/c)	5.5	8	10	16	25
$A = \frac{B - F}{B + F}$	1.00±0.54	0.82±0.18	0.83±0.16	0.56±0.12	0.33±0.17

5. Ξ-PRODUCTION CHANNELS

The Ξ-events were processed through the kinematic fitting program [7] which tried to fit Ξ production hypotheses. Only for about 40% of the Ξ events there was obtained a successful fit to the production vertex. The hypotheses attempted for Ξ production involved an observed Λ^0-decay from the Ξ. The reactions tried and topologies sought are shown in table 4. Passing events were all examined on the scanning table to ensure consistency with observed bubble densities and to resolve ambiguities. In the final sample there were two ambiguous events each of them between two Ξ production reactions. These were assigned to the different channels, weighted by the inverse of the number of fitted reactions. In these events it was not possible to distinguish by ionization between K^+ and π^+.

In table 4 are shown the number of events found, as well as the cross section for different Ξ production channels.

In order to determine the cross section values we used the corrections discussed

Table 4

Cross section for Ξ production reactions

Final state	Production threshold (GeV/c)	a) Observed decay	b) Fraction expected for given topology	Number of events	σ (μb)
$\Xi^-\pi^-\pi^+K^+K^0$	3.098	$\Xi^-(\Lambda),K^0$	2/9	1	1.88±0.92
		$\Xi^-(\Lambda)$	4/9	4,5	
$\Xi^-\pi^-K^+K^+\pi^0$	3.073	$\Xi^-(\Lambda)$	2/3	2,5	0.95±0.32
$\Xi^-\pi^-pK^+\Lambda$	8.079	$\Xi^-(\Lambda)$	2/9	1,5	1.67±1.38
$\Xi^-\pi^-\pi^+p\Xi^0$	7.434	$\Xi^-(\Lambda)$	2/9	0,5	0.57
$\Xi^+p\pi^-K^-\Lambda$	8.079	$\Xi^+(\tilde{\Lambda})$	2/9	1	1.11±2.54 0.89
$\Xi^-\pi^-p\pi^+K^0\Lambda$	8.706	$\Xi^-(\Lambda),K^0$	2/27	1	3.71±8.56 3.00
$\Xi^-\pi^-\pi^-K^+K^+\pi^+$	3.480	$\Xi^-(\Lambda)$	2/3	2	0.76±0.55
$\Xi^-\pi^-\pi^-\pi^+K^+K^0$	3.910	$\Xi^-(\Lambda)$	4/9	2	1.11±0.80
$\Xi^-\pi^-K^+\pi^+\pi^0$	3.883	$\Xi^-(\Lambda)$	2/3	2	0.76±0.55
$\Xi^-K^-\pi^+K^+K^+K^0$	6.344	$\Xi^-(\Lambda)$	4/9	1	0.56±1.27 0.45

a) The particle symbols stand for visible two body decays in the bubble chamber;

b) Rounded decay branching rations are used for simplicity.

above in sec. 2 for each observed decaying particle. In addition, the fitted hypothesis is weighted by an additional factor, w_2, for each unseen neutral strange particle,

$$w_2 = \frac{1}{1 - b_0 + b_0 \exp(-L_{pot}/L_0)},$$

where b_0 is the branching fraction into charged decay product.

The cross section for the first reaction in table 4 can be determined in two independent ways corresponding to the two kinds of events fitting the hypothesis $\Xi^-\pi^-\pi^+K^+K^\circ$ properly weighted. The number listed in table 4, for the cross section is a weighted average of these two values.

The general characteristics of the production of the reactions listed in table 4 are illustrated in figs. 7-16 in which the average momentum of each of the outgoing particle is plotted.

It is noted that in most of the reactions the events tend to have Ξ^- and a strange (K^-) meson going (nearly) backwards in the center of mass and the other mesons being produced forward or nearly symmetrically on the average. P tends to emerge forward in the $\Xi^-(\bar{\Lambda}^\circ)$ reactions and backwards together with $\tilde{\Xi}^+$ in reaction $\tilde{\Xi}^+ p\pi^-K^-\Lambda^\circ$, where Λ° emerges in the beam hemisphere.

We have examined the invariant mass of the $\Xi^-\pi^+$ system for all events from all channel group together and found no evidence for any significant structure in this distribution. Instead of this, the mass distribution of Ξ^-K^+-system, for the same events, shows some small and wide enhancement in the effective mass region from 1.9-2.2 GeV.

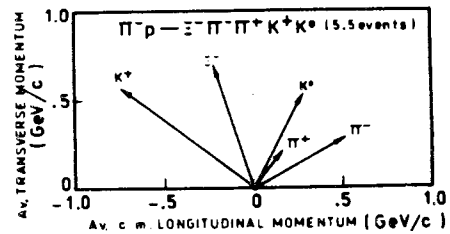

Fig. 7. Average transverse momentum vs. average c.m. longitudinal momentum for the final state particles for reactions listed in table. 4.

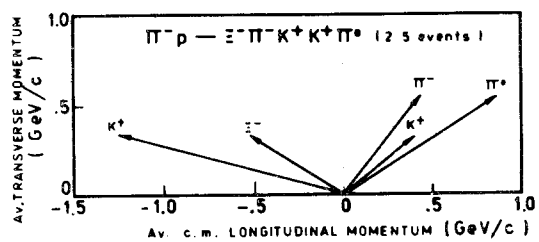

Fig. 8. The same as in fig. 7.

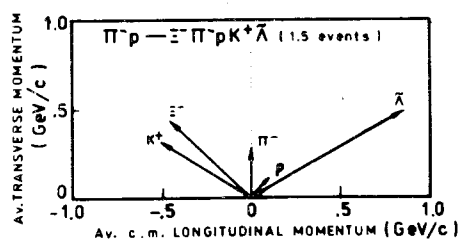

Fig. 9. The same as in fig. 7.

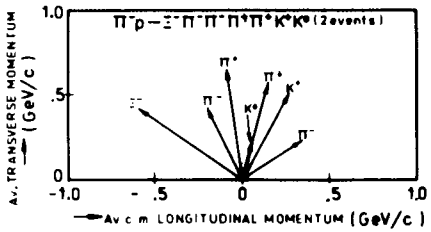

Fig. 10. The same as in fig. 7.

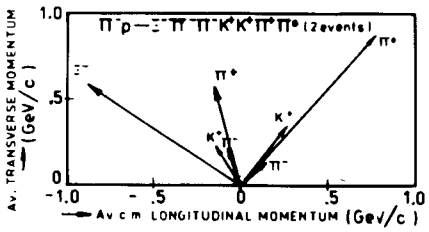

Fig. 11. The same as in fig. 7.

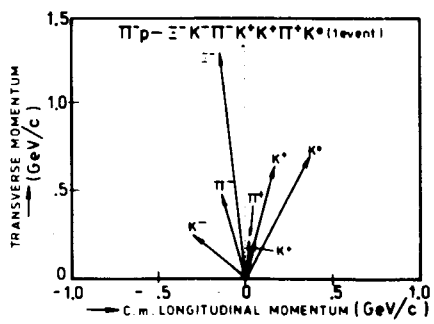

Fig. 12. The same as in fig. 7.

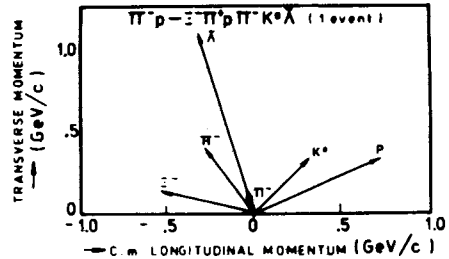

Fig. 13. The same as in fig. 7.

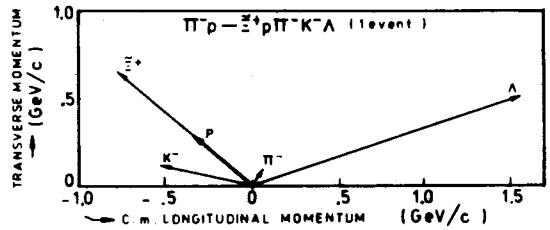

Fig. 14. The same as in fig. 7.

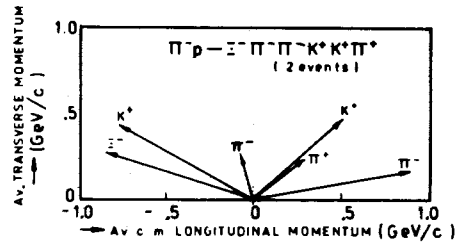

Fig. 15. The same as in fig. 7.

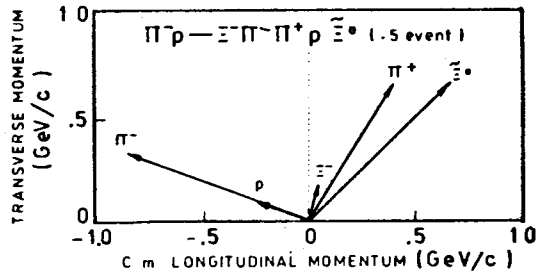

Fig. 16. The same as in fig.7.

ACKNOWLEDGEMENTS

We wish to express out thanks to the CERN for providing us the photographs. We would also like to thank the scanning, measuring and computing staffs in our Laboratories.

REFERENCES

1. Balea E. et al. JINR, 1-8138, Dubna, 1974.
2. Markova N.R. et al. JINR, P10-3768, Dubna, 1968.
3. Lukiantev A.F. et al. JINR, P-1982, Dubna, 1965.
4. Mason C.G., Wohl C.G. Nucl.Phys., B103 1976, B103, p.279.
5. Galbraith et al. Phys.Rev., 1965, 138B, p.913.
   Folley et al. Phys.Rev.Lett., 1967, 19, p.330.
6. Data for Ξ^-'s are from: Wangler T.P. et al. Phys.Rev., 1965, 137B, p.414.
   Dahl Orin. I. et al. UCRL-16978, 1967.
   Bartsch J. et al. Nuovo Cim., 1966, 43, p.1010.
   Dubna - Buharest collaboration, Atayan M.R. et al. Journ.of Nucl.Phys., 1968, 7, p.349.
   Budagov U.A. et al. JINR, P1-4784, Dubna, 1969.
   Fowler W.B. et al. Nuovo Cim., 1959, 11, p.428.
   Wang Kan-Chang et al. JETP, 1961, 40, p.732,
   Bigi A. et al. Nuovo Cim., 1964, 33, p.1265.
   Waters J.W. et al. Nucl.Phys., 1970, B17, p.445.

See also Coca C., Mihul A. Ξ^--Hyperon Production in π^-N-Interactions. (Review), Bucharest, Preprint H.E.-65 (1970).
7. Ivancenco Z.M. et al. JINR, P11-3983, Dubna, 1968.

Received by Publishing Department
on June 12 1978.